Understanding the dechlorination of chlorinated hydrocarbons in the pyrolysis of mixed plastics

Guozhan Jiang[1], D. A. Sanchez Monsalve[2], Peter Clough[3], Ying Jiang[3], Gary A Leeke[1]*

[1]School of Chemical Engineering, University of Birmingham, Birmingham B15 2TT, UK

[2]Recycling Technologies Ltd, Unit B2 Stirling Court, Stirling Road, Swindon SN3 4TQ, UK

[3]School of Water Energy and Environment, Cranfield University, Cranfield, Bedfordshire MK43 0AL, UK

ABSTRACT

The dechlorination of chlorine containing hydrocarbons in pyrolysis vapor is poorly understood. In order to shed new light on the dechlorination mechanism, a model mixture composing of isooctane doped with 2-chlorobutane, 2-chloroethylbenzene, and chlorobenzene was used to study the dechlorination of chlorinated hydrocarbons by alkali adsorption. These three chlorinated hydrocarbons were selected as they can be typically produced from the pyrolysis of mixed plastic waste containing polyvinyl chloride (PVC). The mixture is pumped continuously through a Na_2CO_3 or $CaCO_3$/alumina bed, and GC-MS is used to identify the dechlorination products and to follow the dechlorination reactions. When chlorine is bonded to an aliphatic carbon with an adjacent aliphatic hydrogen, the chlorinated compound firstly undergoes a dehydrochlorination reaction to form HCl and olefins, and subsequently the HCl is reacted with the alkali in the absorbents. In our experiments, 2-chlorobutane is converted to 2-butene, and 2-chloroethylbenzene is converted to styrene. The formation of HCl and subsequent reaction with

* Corresponding author. Telephone +44 (0) 121 414 4977; Email: G.A.Leeke@bham.ac.uk

alkali components in the absorbent is verified by IR spectroscopy and XRD. In the presence of an alkali, the aliphatic chlorinated hydrocarbons underwent dechlorination at a temperature of 180ºC. The removal of chlorine from aromatic chlorinated compounds operates in a different mechanism, in which the C-Cl bond scission is promoted significantly by the presence of alumina and hydrocarbon medium. It was found that chlorobenzene undergoes dechlorination forming phenol and benzene.

INTRODUCTION

Pyrolysis recycling of plastic waste is becoming recognized as a viable route for the circular plastic economy where the pyrolysis oil can be cracked and further refined for new plastic production. A problem associated with pyrolysis recycling of mixed plastic waste is the presence of halogen containing components in the waste stream. The primary source of halogens is polyvinyl chloride (PVC), the pyrolysis of which produces HCl and chlorinated hydrocarbons. For downstream processing of the pyrolysis oil in existing petrochemical plants, chlorine content in the pyrolysis oil must be reduced to less than 10 ppm to prevent unit corrosion.[1]

In commercial pyrolysis of mixed plastic waste containing PVC, a low-temperature pyrolysis between 300 and 330°C is used to remove chlorine via dehydrochlorination reactions.[2] Chlorine cannot be completely removed in this stage since some isolated chlorine atoms are locked inside the remaining structures due to cyclisation and crosslinking with increasing extent of reaction.[3] Westerhout et al. [4] estimated that at least 2% of chlorine went to the next pyrolysis stage. Steam assisted low-temperature pyrolysis can enhance the dehydrochlorination reaction.[5, 6] Recently, Nishibata et al. [7] investigated dechlorination of PVC plastics using a combination of superheated steam and CaO to achieve a higher extent of dechlorination. Wet treatment in glycol/NaOH mixture is also an effective method to remove chlorine instead of low-temperature pyrolysis pre-treatment.[8, 9] Although these new technologies have been developed, capture of chlorine by solid adsorbents during pyrolysis or in subsequent upgrading plastic derived oil is still the dominant technology for reducing chlorine to the required criteria because of its easy operation and low cost.[10]

Alkali adsorbents are widely used either in the pyrolysis reactor or down-stream adsorption. In 1990s, Hinz et al. [11] carried out a pilot plant scale study of chlorine adsorption by ammonia when running the Hamburg fluidized bed plastic recycling process, which pyrolyzes plastic waste at around 700°C to produce gaseous products. The feedstock had a chlorine content of 5% (wt.), whereas the chlorine content in the derived oil was reduced to between 10 ppm to 1000 ppm. The use of limestone (CaO) in the bed was not recommended in this process because of the difficulty in separating the by-product $CaCl_2$ and the bed material. However, the use of limestone or calcium carbonate in the bed can effectively remove chlorine in the produced oil. Cho et al. [12] used lime, $Ca(OH)_2$ or oyster shell (consisting mainly of $CaCO_3$) to adsorb chlorine when

3

pyrolyzing mixed plastics containing 1.13% (wt) chlorine in a 1 kg/h fluidized bed reactor at a temperature range between 680°C and 780°C. The resultant oil had a chlorine content of 50 ppm. Bhaskar et al. [13] used $CaCO_3$ supported on carbon to adsorb both chlorine and bromine in a batch reactor for pyrolysis of plastic waste at 430°C. The feedstock contained 10% (wt) PVC and 10% (wt) brominated polystyrene giving a Cl content of 50000 ppm and a Br content of 10000 ppm. The adsorbent was placed downstream for contacting the pyrolysis vapour. A halogen free liquid was produced when the ratio of Ca-C (prepared by the calcination of 90 wt% $CaCO_3$ and 10 wt% phenol) to feedstock was 0.4. The difference between the adsorption efficiency in Cho et al's work[12] and Bhaskar et al's work[13] may be due to the effect of temperature. It was shown that the binding capacity of CaO to HCl peaked at 500-600°C in a fluidized bed.[14] Daoudi and Walters [15] showed that CaO conversion levels increased at lower temperatures, because high-temperature results in sintering and thus higher grain diffusion resistance.

Metal oxides are another type of adsorbent for chlorine removal in the pyrolysis of mixed plastic waste. Successful examples include the use of iron oxides such as Fe_2O_3 supported on carbon[16] or SiO_2[17], Fe_3O_4 [18], and FeOOH.[19] Over these adsorbents, the adsorption is often carried out at around 300-350°C with a chlorine conversion of greater than 80%, with iron oxide being converted to iron chloride when iron oxides were used. In batch operation with red mud (composed mainly of Fe_2O_3), Lopez et al [20] reported that the chlorine content in the liquid stream reduced from 2000 ppm to 10 ppm when processed at 325°C with a dwell time of 30 min. Other metal oxides have also been tested to adsorb chlorine from mixed plastics-derived oil such as ZnO and MgO and achieved limited success.[19]

In these reports, the nature of the chlorine was not clearly stated. The mechanism for the adsorption of HCl by alkali or metal oxides is clearly an acid-base neutralisation reaction. However, the dechlorination of the chlorinated hydrocarbons, has not so far been elucidated. In this work, we aim to understand how the chlorinated hydrocarbons can be dechlorinated by alkali adsorption, especially in the presence of hydrocarbons. An insight into dechlorination of chlorinated hydrocarbons will be beneficial for designing effective chlorine sorbents. Efficient adsorbents can both be used to adsorb chlorine from pyrolysis vapour or from pyrolysis oil and therefore provide a chlorine free oil for downstream processing, aiding in the overall success of plastic-to-fuel or plastic-to-plastic technology.

In a commercial plastic waste pyrolysis system, the chlorinated hydrocarbons are mixed with other hydrocarbons in the pyrolysis vapour. We investigated this problem using a model system composing of isooctane doped with the two types of chlorinated compounds, which were elected from the list of chlorinated hydrocarbons obtained from pyrolysis of plastic waste containing PVC. A systematic investigation by McNeill et al. [21] and Miranda et al. [22, 23] provides a detailed list of the chlorinated hydrocarbons that can be produced during pyrolysis of PVC or mixed plastic waste containing PVC. The chlorinated hydrocarbons in the list can be classified into two categories: aliphatic, in which the chlorine atom is bonded with an aliphatic carbon, and aromatic, in which the chlorine atom is bonded with an aromatic carbon. Three chlorinated hydrocarbons were elected from the list of Miranda et al. [22, 23]: 2-chlorobutane (aliphatic), 2-chloroethylbenzene (aliphatic with a benzene ring), and chlorobenzene (aromatic). The iso-octane was selected to represent the light-end compounds in the plastic-derived oil.

EXPERIMENTAL

Chemicals

The three chlorinated hydrocarbons, 2-chlorobutane ($\geq$ 99%), 2-chloroethylbenzene ($\geq$ 99%) and chlorobenzene (anhydrous, 99.8%), and the hydrocarbon medium 2,2,3-trimethylpentane (isooctane) (anhydrous, 99.8%) were purchased from Sigma-Aldrich (UK) and used as received. The adsorbents used in this work were Na_2CO_3 and $CaCO_3$ from Sigma-Aldrich UK (Anhydrous, $\geq$ 99.5%) and Longcliffe UK ($\geq$98%), respectively, and used as received. Alumina pellets (2 mm) were obtained from Fisher Scientific UK and used as the support. Silicon carbide (SiC) (-200 mesh) obtained from Sigma-Aldrich UK was used as the support for the adsorption bed.

Experimental procedure

A schematic diagram of the experimental rig is shown in Figure 1. The continuous flow rig consisted of a feedstock bottle (5L), a HPLC pump (Jasco PU-1586 Intelligent Prep Pump), a tubular flow reactor (600 mm × ½" 316 stainless steel tube from Swagelok), a condenser, a gas-liquid separator, a sampling valve, and a collection bottle (5L). The tube reactor was placed vertically in a Carbolite™ tube furnace (Model EVA 12/450).

The reactor had three sections: SiC (-200 mesh, Sigma-Aldrich) in the lower part, the absorbent bed in the middle (in the uniform heating zone), and SiC on top of the adsorbent bed. A thin layer of glasswool was placed to separate each section and facilitate later collection of the adsorbent. SiC was used to support the adsorption bed and enabled a uniform wetting of the bed.[24] Before an adsorption experiment, the system was pressurized with nitrogen to 10 bar for a gastight test and then flushed using nitrogen to remove air in the system. After nitrogen flushing, the adsorption column was heated to a desired temperature, which was monitored by the thermocouples T1 and T2. When the temperature reached the desired value and stabilized for about 30 minutes, the HPLC pump was started to pump isooctane solution containing the chlorine compounds each with a concentration of 10000 ppm (wt) from the feedstock bottle into the top of the adsorption column. The vapour coming out of the bottom of the bed was condensed in the condenser, and then went to the collection bottle after a gas-liquid separator. The non-condensable gas was vented to an extraction system.

After an adsorption experiment, Na_2CO_3 or $CaCO_3$ were separated from the alumina. The separated adsorbent was kept in a pre-dried glass vial for further analysis. It was easy to perform the separation since both Na_2CO_3 and $CaCO_3$ were fine particles, and alumina was in pellet form.
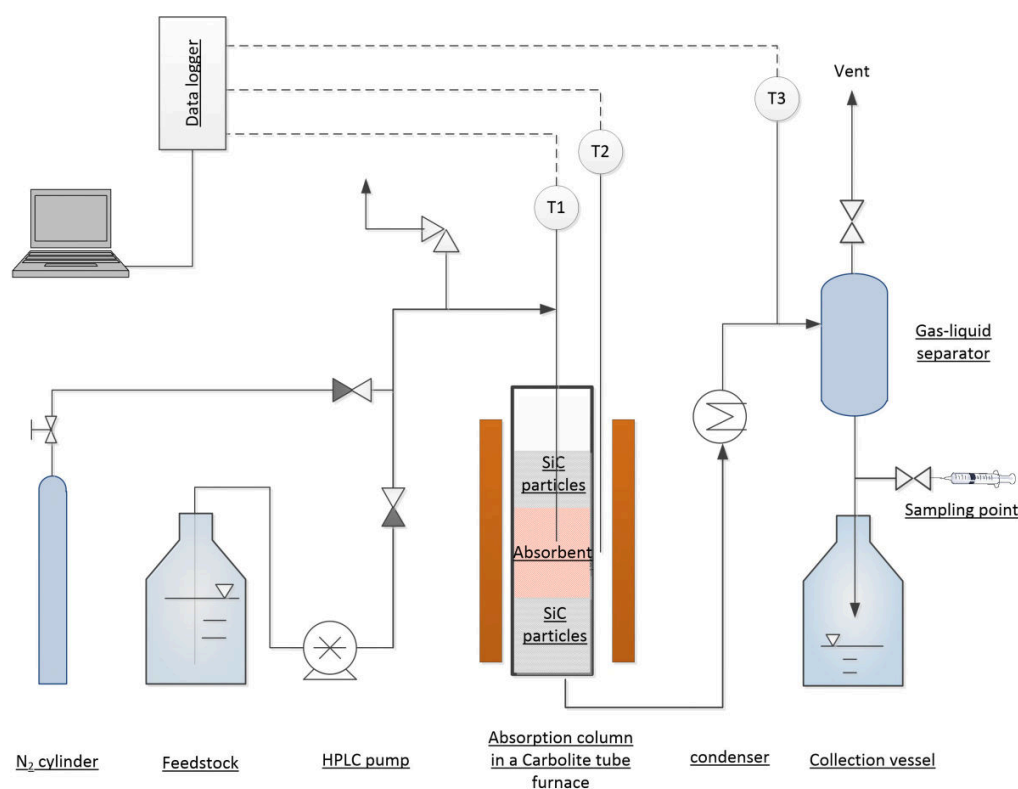
Figure 1. A schematic diagram for the continuous flow adsorption rig

Two types of experiments were conducted: staged heating adsorption and isothermal adsorption. In staged heating adsorption, the adsorbent bed was heated to a temperature and then kept at that temperature for 10 min, and then the temperature of the column was increased to higher temperatures in 20°C steps and held isothermally for 10 minutes at each step to about 550°C. A solution containing 10000 ppm (wt) of single or mixed chlorinated hydrocarbons in isooctane was passed through the bed at a liquid flow rate of 2ml/min. This flow rate was determined by the liquid space velocity (LSV) so that sufficient residence time was provided for the dechlorination process (Figures S1 to S2). Samples were taken at each temperature step from the outlet liquid and were subsequently analysed by GC test to determine the reaction products. The staged adsorption experiment was used to determine the adsorption temperature of a chlorinated hydrocarbon compound.

In the isothermal adsorption experiment, the adsorbent bed was heated to a pre-determined temperature and kept at that temperature. A chlorinated hydrocarbon in isooctane solution with a concentration of 10000 ppm (wt) each passed through the bed at a flow rate of 2 ml/min until a

breakthrough point was reached, where chlorinated hydrocarbons were detected in the exit solution. The isothermal adsorption experiment was used to determine the adsorption capacity of the adsorbent.

The adsorption process of a chlorinated hydrocarbon was followed using GC/MS by monitoring the ratio of outlet to inlet peak area of the corresponding chlorinated hydrocarbons, which is equivalent to the ratio of the outlet to inlet concentration. The measurement error of the peak area is less than 6% under the conditions of the GC/MS, which is propagated to an error of 8% of the area ratio.

Analysis procedure

The reaction products were identified and quantified using GCMS. The GCMS consists of a Perkin Elmer Clarus 680GC hyphenated with a Clarus SQ8T mass spectrometer, equipped with an auto-sampler and a 30 m long Perkin Elmer Elite-5 capillary column. A full scan mode was used and then the peak areas of proper quantitation ions were measured for the compounds of interest.

Infrared spectroscopy was used to observe the changes in the vibrational spectra of the adsorbent after absorbing the chlorinated hydrocarbons. The adsorbents were crushed into powder form before analysis. The spectra were acquired using a Shimadzu Tracer 100 FTIR-ATR facility over a spectral range of 4000–600 cm^{-1} with 16 times of scan and a resolution of 4 cm^{-1}.

The presence of inorganic chlorinated compounds in the adsorbents was determined using X-ray diffraction (XRD) on a Siemens D5005 diffractometer with Cu Kα radiation ($\lambda = 1.5418$ Å) at room temperature. The XRD was operated at 40 kV and 40 mA with the scan rate of 0.04º/s over the 2θ range from 20-90º. Diffrac.EVA V4.1 was used to analyse the XRD patterns.

RESULTS AND DISCUSSION

Thermal effect on dechlorination

A blank experiment was conducted in the absence of adsorbents to investigate the dechlorination behaviour of these chlorinated hydrocarbons at elevated temperatures in the isooctane medium,

in which the adsorbent bed consisted of only SiC, a chemically inert material[25]. The variation of GC peak area of the chlorinated hydrocarbons and their decomposition products in the outlet stream are plotted against temperature in Figure 2.
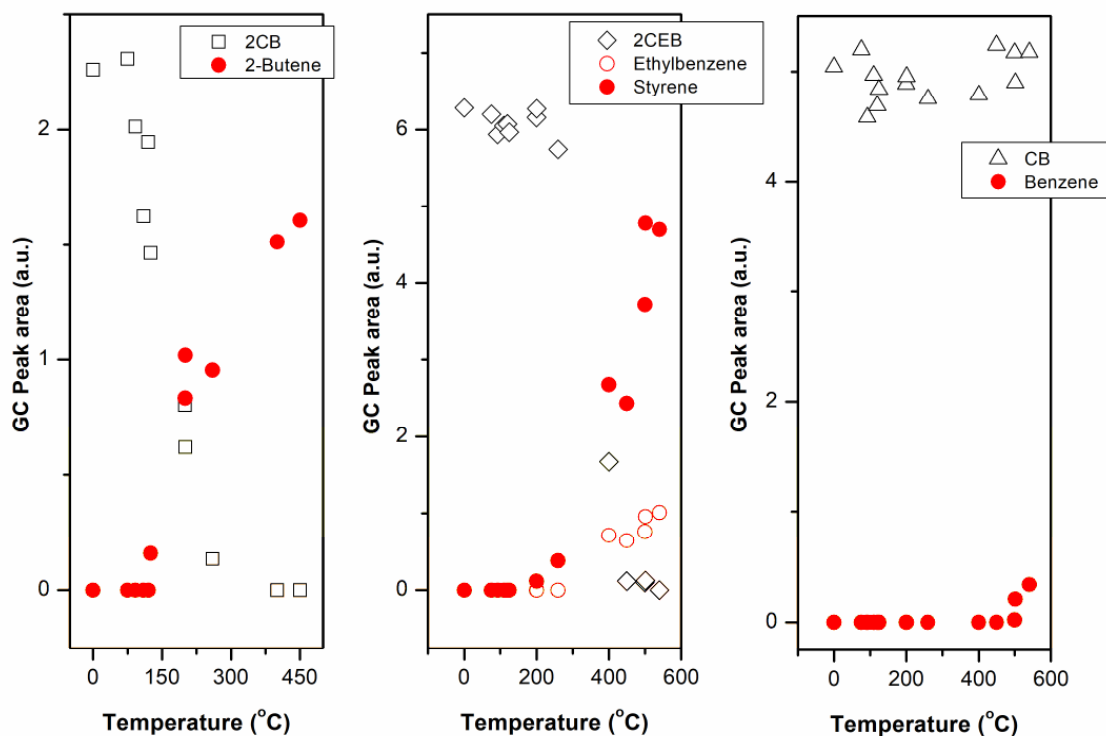

Figure 2. The influence of temperature on the thermal decomposition of chlorinated hydrocarbons in isooctane. The concentrations of 2-chlorobutane (2CB), 2-chloroethylbenzene (2CEB) and chlorobenzene (CB) in the inlet stream were 10000 ppm (wt.), respectively. No other compounds were detected in the GC chromatogram.

For 2-chlorobutane solution passing through the reactor, only 2-chlorobutane was detected at the outlet stream before 125°C. 2-Butene was first detected at 125°C, which is clearly the dehydrochlorination product of 2-chlorobutane as shown in Scheme 1. With increasing temperature, the concentration of 2-chlorobutane decreases and 2-butene increases rapidly. When the temperature reaches 200°C, 2-chlorobutane concentration in the outlet stream drops to about 50% of the inlet concentration. When the temperature reaches 350°C, 2-chlorobutane is not detectable in the outlet stream, and the concentration of 2-butene reaches a maximum value.

At about 200ºC, styrene is detected in the outlet stream for 2-chloroethylbenzene solution, which is clearly the dehydrochlorination product of 2-chloroethylbenzene as shown in Scheme 2. With increasing temperature, the concentration of 2-chloroethylbenzene in the outlet stream decreases and styrene concentration increases correspondingly. At 400ºC, the concentration of 2-chloroethylbenzene drops to about 30% of that of the inlet solution. In the meantime, ethylbenzene is detected in the outlet stream, which should be a secondary reaction product of styrene. However, 2-chloroethylbenzene can still be detected in the outlet stream even at 550ºC, although the concentration is only about 2% of that in the inlet concentration. It can be seen here that 2-chloroethylbenzene is more difficult to be dehydrochlorinated.
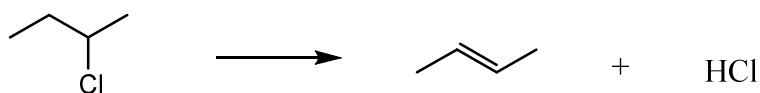
Scheme 1. Dehydrochlorination of 2-chlorobutane.
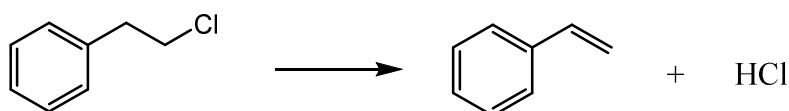
Scheme 2. Dehydrochlorination of 2-chlorobutane.

No decomposition products are detected until 500ºC for chlorobenzene solution. At 500ºC, a trace amount of benzene is detected in the outlet stream, indicating that there is a decomposition of chlorobenzene at this temperature. However, the extent of decomposition is quite small. When the temperature is raised up to 550ºC, the concentration of chlorobenzene in the outlet stream is similar to that at 500ºC. Cullis et al. [26] reported a minimum thermal decomposition temperature of 740ºC for chlorobenzene, mainly via stripping of the aromatic rings forming benzene. Li et al. [27] reported that chlorobenzene does not undergo decomposition below 600ºC in an inert gas, but there is a small extent of decomposition in hydrogen at 500ºC. In this work, the reaction medium is isooctane, which may promote a thermal decomposition at around 500ºC producing trace amount of benzene, as discussed in the following mechanism section.

Na$_2$CO$_3$ effect on dechlorination

From the above results, where only thermal treatment was used, the chlorine in 2-chlorobutane and in 2-chloroethylbenzene can be removed via dehydrochlorination starting from 125°C and 200°C, respectively, whereas the chlorine in chlorobenzene cannot be removed below 500°C. The chlorine removed would be in the form of HCl and exit from the outlet stream. An alkali adsorbent can therefore be used to adsorb the HCl. In order to test the effect of alkali adsorbents, isothermal adsorption experiments were performed at various temperatures. Isothermal adsorption of the three chlorinated hydrocarbons in isooctane was conducted using a mixture of Na$_2$CO$_3$ /Al$_2$O$_3$ pellets. A typical GCMS chromatogram is shown in Figure 3 for the adsorption at 180°C and 450°C, and typical adsorption curves are plotted in Figure 4. The adsorption curve for other temperatures are similar and shown in Figures S3-S6.

Figure 3 shows that there are three peaks for the three chlorinated hydrocarbons in the inlet stream (Figure 3A). After passing through the adsorption bed at 180°C (Figure 3B), the peak for chlorobenzene remains, but the peaks for 2-chlorobutane and 2-chloroethylbenzene disappear. Instead, two new peaks appear at 1.53 min and 5.37 min, which were identified as 2-butene and styrene, respectively. According to the products, 2-chlorobutane and 2-chloroethylbenzene undergo dehydrochlorination reactions as in the blank test.

When the solution passes through the adsorption bed at 450°C (Figure 3C), three other peaks appear at 2.25 min, 4.80 min and 7.34 min, which were identified as benzene, ethylbenzene and phenol, respectively. According to structural similarity, ethylbenzene is a reaction product of styrene at 450°C. Benzene and phenol are the reaction products of chlorobenzene. Besides these peaks attributed to the adsorption of chlorinated hydrocarbons, there are small peaks at 2.02 min and 1.44 min. These peaks are light aliphatic hydrocarbons (butane and isobutane, 1.44 min, 1.42 min), which are attributed to cracking of isooctane.[28]
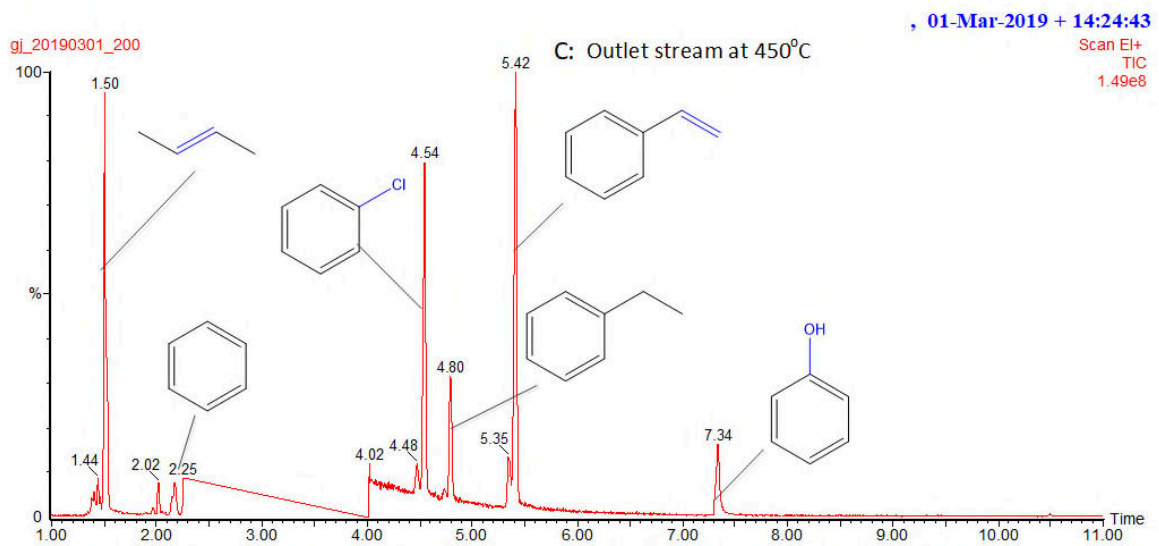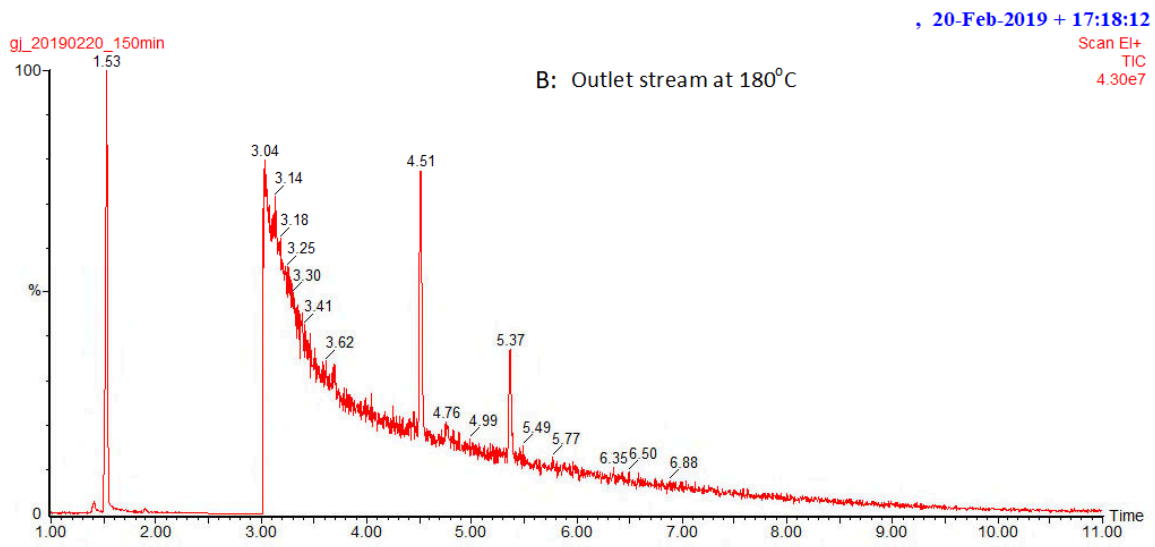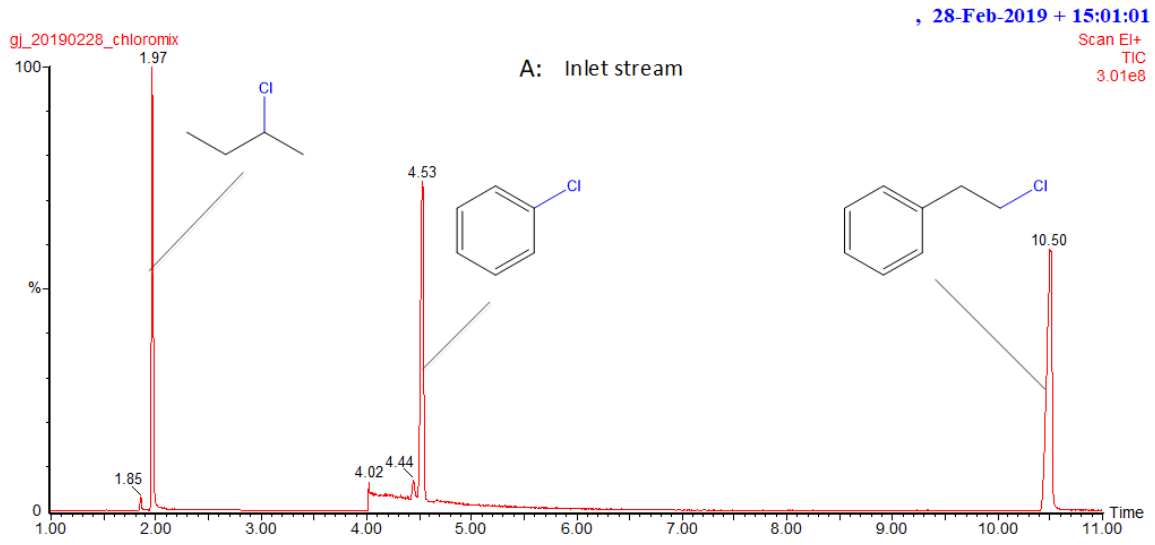
gj_20190228_chloromix

A: Inlet stream

Scan EI+
TIC
3.01e8

1.97

1.85

4.53

4.02 4.44

10.50

gj_20190220_150min

B: Outlet stream at 180°C

Scan EI+
TIC
4.30e7

1.53

3.04
3.14
3.18
3.25
3.30
3.41
3.62
4.51
4.76 4.99
5.37
5.49 5.77
6.35 6.50
6.88

gj_20190301_200

C: Outlet stream at 450°C

Scan EI+
TIC
1.49e8

1.50

5.42

4.54

4.80

1.44
2.02 2.25
4.02 4.48
5.35
7.34

Figure 3. Typical GCMS chromatograms of inlet (A) and outlet stream (B and C) for the adsorption of the chlorinated hydrocarbons on Na_2CO_3/Al_2O_3 at 180^oC (B) and 450^oC (C). The liquid flow rate was 2 ml/min. Initial concentrations of the chlorinated hydrocarbons were 10000ppm (wt), respectively.

As shown in Figure 4, 2-chlorobutane and 2-chloroethylbenzene are not detected in the outlet stream for the first 50 min at 180^oC. After 50 min, both 2-chlorobutane and 2-chloroethylbenzene are detected with a concentration of 5% of that of the inlet concentration, and then the concentrations of the two aliphatic chlorinated hydrocarbons increases gradually. This indicates that the Na_2CO_3 bed starts to become saturated at about 50 min on stream.
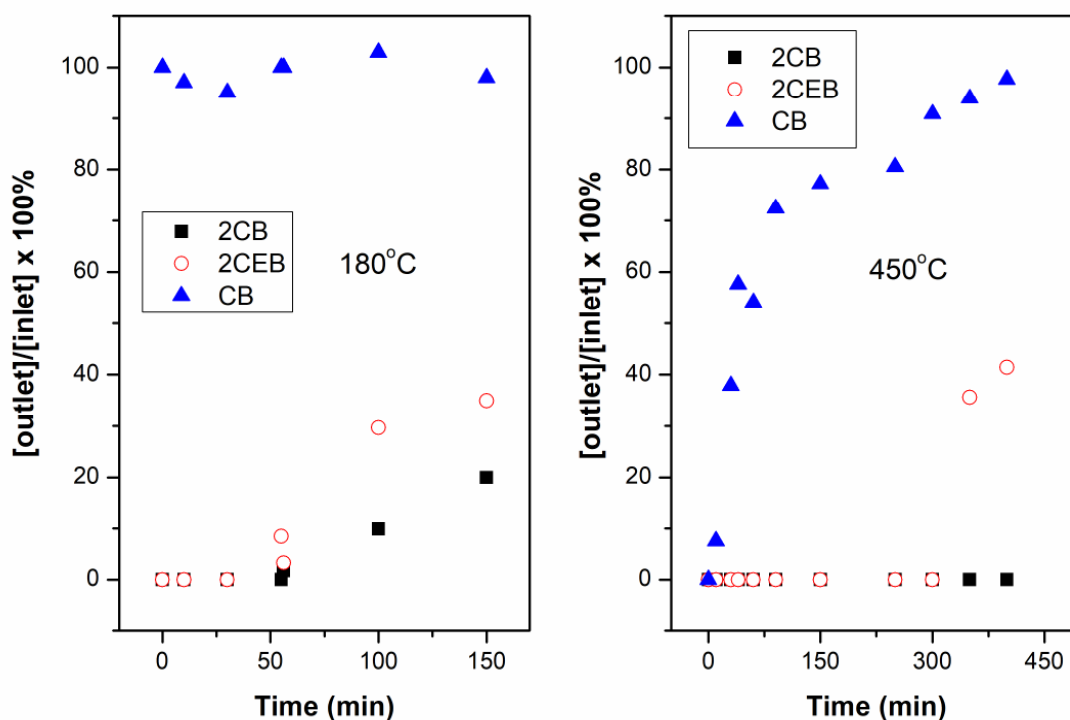

Figure 4. Co-adsorption of the three chlorinated hydrocarbons in isooctane at different temperatures. The adsorbent bed consisted of a mixture 3 g Na_2CO_3 and 12 ml (4.72 g) alumina pellets for the adsorption at 180^oC and a mixture of 10 g Na_2CO_3 and 30 ml (11.8 g) alumina pellets for the adsorption at 450^oC, and the inlet liquid flow rate is 2 ml/min. The concentrations of 2-chlorobutane (2-CB), 2-chloroethylbenzene (2-CEB) and chlorobenzene (CB) were 10000 ppm (wt), respectively.

For an adsorption temperature of 450°C, the adsorption bed consists of 10 g Na_2CO_3 and 25 ml (9.8 g) Al_2O_3 pellets. This increased mass allowed the adsorption behaviour to be observed over a longer time. Both 2-chlorobutane and 2-chloroethylbenzene were not detected for the first 300 minutes. After about 300 minutes, 2-chloroethyl benzene was detected at the outlet, indicating that the adsorbent starts to become saturated. However, the breakthrough time of 2-chlorobutane does not appear when compared to the test at 180°C. This is most probably due to the chemical equilibrium strongly favouring the formation of 2-butene at 450°C. The reaction will proceed according to Scheme 1 in the absence of Na_2CO_3. The reaction equilibrium constant of Scheme 1 at 450°C was calculated according to Equation 1.

$$K = \ln\left(\frac{-\Delta G_r}{RT}\right)$$ (1)

Where ΔG_r is the Gibbs energy change of the reaction, R is the gas constant, and T is the temperature. According to the thermochemical data of the reactant and products (from Lange's Handbook of Chemistry), K = 206 at 450°C. This suggests that the equilibrium concentration of 2-butene is only 6% to that of 2-chlorobutane. Consequently, the breakthrough time may not be observed at this point. The favourable presence of 2-butene for the equilibrium of 2-chlorobutane and 2-butane and HCl can also be seen from Figure 2, where 2-chlorobutane was not detectable at 450°C in the absence of any adsorbents.

It can be seen that the products are the same whether the two aliphatic chlorinated hydrocarbons pass through a bed of Na_2CO_3 or not. Under both conditions, 2-butene and styrene are formed, respectively. The difference between the two conditions is that the dehydrochlorination temperature was lowered when Na_2CO_3 was used. It has been shown in the blank test that dehydrochlorination reactions of 2-chlorobutane start at about 125°C. At 180°C, about 50% of 2-chlorobutane was thermally converted to 2-butene, as shown in Figure 2. When 2-chlorobutane passes through an adsorption bed of Na_2CO_3 with the same space velocity, all the 2-chlorobutane is converted to 2-butene. There was no thermal dehydrochlorination of 2-chloroethylbenzene at 180°C, but the conversion of 2-chloroethylbenzene to styrene is completed in the presence of Na_2CO_3 at this temperature. An overall reaction as shown in Schemes 3 and 4 can be drawn for the dehydrochlorination in the presence of Na_2CO_3.
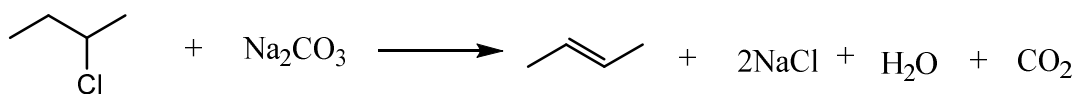
Scheme 3. Dehydrochlorination of 2-chlorobutane in the presence of Na_2CO_3.
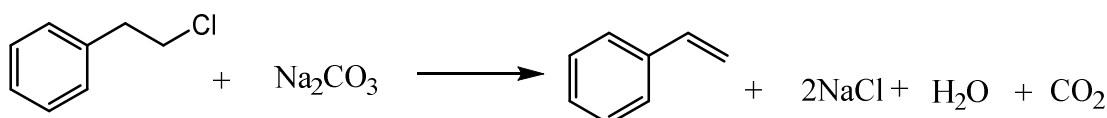
Scheme 4. Scheme 3. Dehydrochlorination of 2-chlorobutane in the presence of Na_2CO_3.

The change of the mass of the adsorbent before and after adsorption experiments was calculated using Equation (1) according to Schemes 3 and 4, which indicates that when 1 mole of the adsorbate is converted, the increase in the mass of the adsorbent is equivalent to the mass difference of 2 mole Cl^- and 1 mole of CO_3^{2-}.

$$w = (\frac{V\rho C_{2CB}}{MW_{2CB}} + \frac{V\rho C_{2CEB}}{MW_{2CEB}}) \times (71 - 60)/2 \tag{1}$$

Where V is the solution volume passing through the adsorption bed, ρ is the density of isooctane, C is the concentration of adsorbate, and MW is the molar mass, 71 is the relative molar mass (RMM) of $2Cl^-$, and 60 is the RMM of CO_3^{2-}. The subscripts 2CB and 2CEB represents 2-chlorobutane and 2-chloroethylbenzene, respectively.

The results are, compared with the measured mass changes in Table 1. It can be seen that for 2-chlorobutane and 2-chloroethylbenzene, the mass change of the adsorbent is very close to the calculated mass change according to the schemes. It can therefore be considered that the dechlorination process is via dehydrochlorination reactions. However, there is a large discrepancy between the mass change and the calculated mass change. The calculation of chlorobenzene adsorption was based on the exchange of the chlorine and oxygen atom using Equation (2) and is discussed in the following mechanism section.

$$w = (\frac{V\rho C_{CB}}{MW_{CB}}) \times (35.5 - 16) \tag{2}$$

Where V is the solution volume passing through the adsorption bed, ρ is the density of isooctane, C is the concentration of adsorbate, and MW is the molar mass, 35.5 is the RMM of chlorine, and 16 is the RMM of oxygen. The subscripts CB represents chlorobenzene.

Table 1. Comparison of adsorbent mass changes and calculated mass changes according to Schemes 3 and 4.

Exp.#	Adsorbent	Temperature (^{o}C)	adsorbate	Measured mass change (g)	Calculated mass change (g)
220	Na_2CO_3	180	2CB + 2CEB	0.1154	0.0956
227	Na_2CO_3	250	2CB +2CEB	0.5202	0.5792
329	Na_2CO_3	450	CB	0.3402	0.6775

The isothermal adsorption of chlorobenzene is quite different to those of the two aliphatic chlorinated hydrocarbons. At 180°C, the outlet concentration of chlorobenzene does not show a significant change compared with that of the inlet stream, which indicates that chlorobenzene cannot be dechlorinated at this temperature. At 450°C, the concentration of chlorobenzene of the outlet stream drops to about 5% of the inlet stream concentration at the start, and then increases gradually to nearly the same as that of the inlet stream concentration over 400 min, indicating that chlorobenzene can be dechlorinated at 450°C. However, the breakthrough time is much shorter than that of the two aliphatic chlorinated hydrocarbons.

It can also be seen from Figure 4 that the adsorption of 2-chlorobutane and 2-chloroethylbenzene is not affected by the adsorption of chlorobenzene. Although the adsorption of chlorobenzene slows down gradually, the adsorption of the two chlorinated compounds continues without any interruption. This behaviour indicates that two different mechanisms of dechlorination are operating for the adsorption of 2-chlorobutane and 2-chloroethylbenzene, and for the adsorption of chlorobenzene. This is reasonable since chlorobenzene has no aliphatic hydrogen adjacent to chlorine to affect its ability to leave and form HCl and an olefin. The very short breakthrough time for chlorobenzene suggests that the adsorption of chlorobenzene proceeds mainly on the surface with the interior of the adsorbents is probably not accessed. When the Na_2CO_3 surface is used up and the interior is covered by the chemisorbed product, the dechlorination reaction stops.

The dechlorination of chlorobenzene proceeds at 450°C in this study. This temperature is much lower than those reported in the previous work of Parrett et al. [29] They reported a minimum adsorption temperature of 600°C for the adsorption of chlorobenzene on Na_2CO_3 in the absence of a carrier gas. Li et al. [27] conducted chlorobenzene adsorption on nanoscale CaO using various carrier gases. When the carrier gas was helium, adsorption was detected at 700°C, however when the carrier gas was hydrogen, the adsorption was detected at 500°C, with an extent of decomposition of about 10%. The reduction in adsorption temperature may be attributed to the reduction by hydrogen. These research works indicate that the adsorption medium has an influence on the reaction temperature. The much lower reaction temperature of adsorbing chlorobenzene in this work suggests that the presence of alumina and isooctane has promoted the adsorption. In the following, the effects of alumina and Na_2CO_3 on the dechlorination of chlorobenzene is investigated to seek deeper insight into the adsorption of chlorobenzene.

Dechlorination of chlorobenzene

Figure 5 shows the chlorobenzene concentration ratio of outlet to inlet stream with adsorption temperature when a solution of chlorobenzene in isooctane was passed through different adsorbent beds. It can be seen that alumina and Na_2CO_3 has no dechlorination effect on chlorobenzene from room temperature to 550°C when they are used alone. However, chlorobenzene is dechlorinated when the solution passed through a bed of Na_2CO_3 mixed with alumina at about 300°C. The dechlorination products are benzene and phenol, as shown in Figure 6, a typical chromatogram for the adsorption process. The higher the temperature, the more dechlorination takes place; at 410°C, the dechlorination is about 90%. It can be concluded that Al_2O_3 combined with Na_2CO_3 can enhance the dechlorination of chlorobenzene. Further increases in temperature results in an increase in the outlet concentration of chlorobenzene. This can be considered a breakthrough point of the adsorption bed of Na_2CO_3/alumina indicating when all the alkali has been consumed.
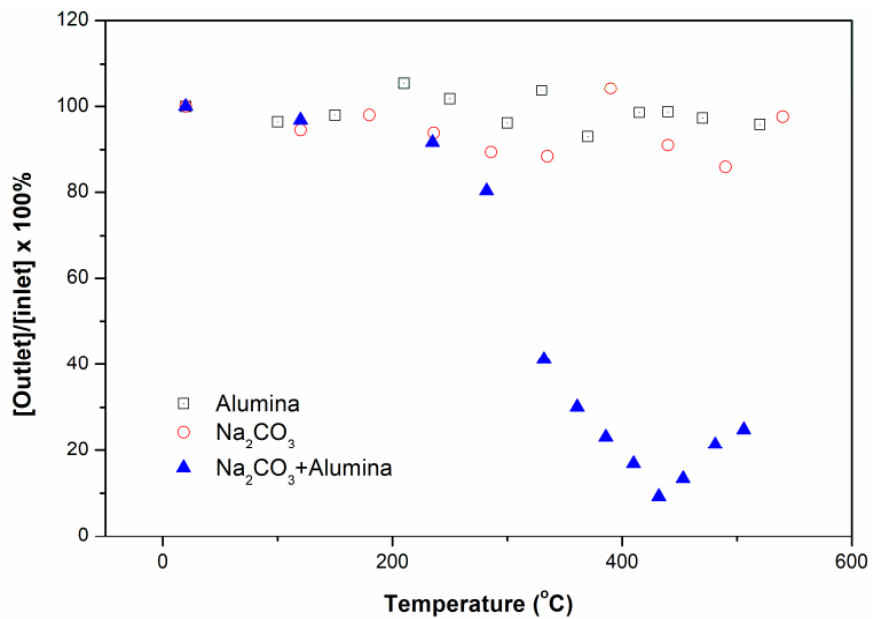
Figure 5. Dechlorination of chlorobenzene over different adsorption beds and temperatures. The concentration of chlorobenzene in isooctane was 10000 ppm (wt.). The inlet liquid flow rate was 2 ml/min. The bed consisted of 3 g Na_2CO_3 or 12 ml (4.7 g) alumina or their mixture.
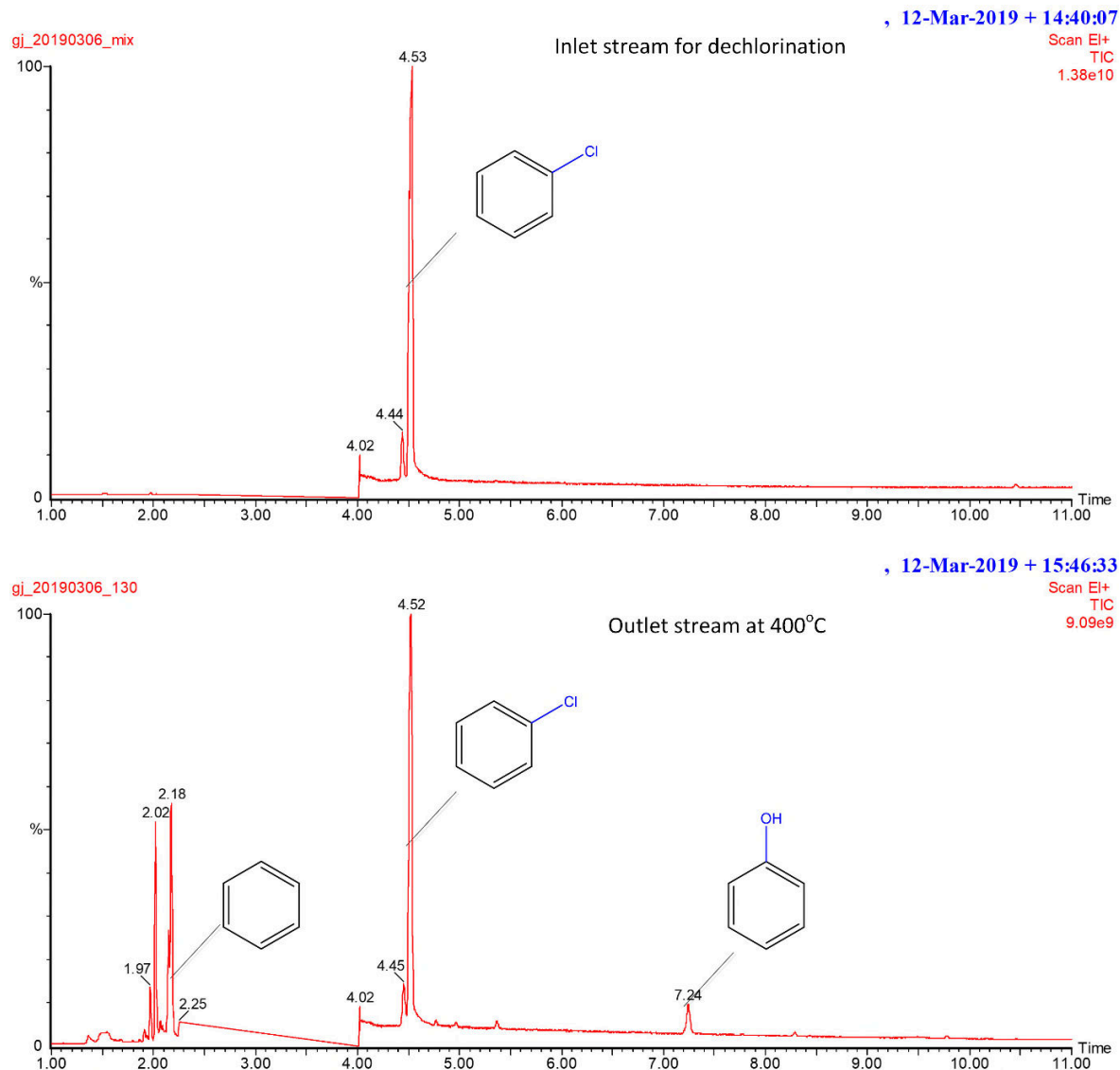
Figure 6. GCMS chromatogram of inlet and outlet stream for the adsorption of chlorobenzene at 400ºC. The liquid flow rate was 2 ml/min. Initial concentration of chlorobenzene was 10000 ppm (wt).

In order to further confirm the effects of alumina, $CaCO_3$ was used to conduct similar experiments to those of Na_2CO_3. It can be seen in Figure 7 that $CaCO_3$ alone does not dechlorinate chlorobenzene. When $CaCO_3$ and alumina were used together, chlorobenzene was dechlorinated. For $CaCO_3$, the dechlorination starts at about 400ºC, which is about 80ºC higher than that of Na_2CO_3. It should be noted that breakthrough does not appear for $CaCO_3$ since the

bed contains more than double the amount of alkali in order to observe the effect of varying alkali amount.
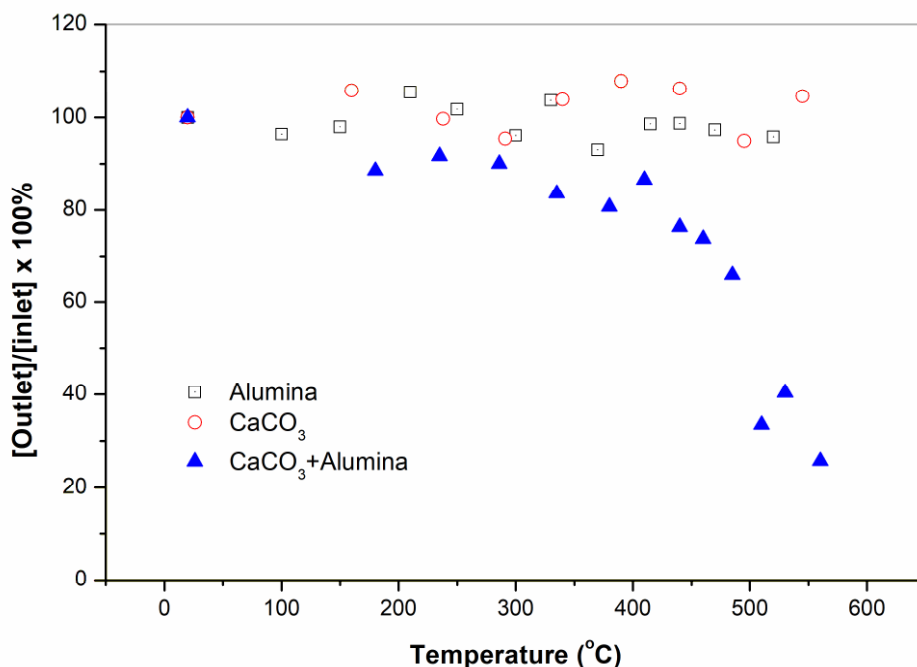

Figure 7. Dechlorination of chlorobenzene over different adsorption beds and temperatures. The concentration of chlorobenzene in isooctane was 10000 ppm (wt.). The inlet liquid flow rate was 2 ml/min. The bed consisted of 6 g $CaCO_3$ or 12 ml (4.7 g) alumina or their mixture.

The IR spectra of the Na_2CO_3 before and after the adsorption experiments are shown in Figure 8. Na_2CO_3 has three characteristic adsorption band at 1417, 877 and 702 cm^{-1}, which are attributed to in-, out-plane bending and asymmetrical stretching vibration of O-C-O bond, respectively. After the adsorption of chlorobenzene, the positions of these bands do not change, but the intensities decrease significantly. It is well known that the band intensity is dependent upon the concentration. This indicates the concentration of O-C-O bond decreases after adsorption of chlorobenzene, and thus some Na_2CO_3 is consumed. From the IR spectra, the conversion of Na_2CO_3 is about 40% (atom basis) after the breakthrough point is reached. It can be inferred that a dispersion of alkali on a large surface carrier may enhance the efficiency of the adsorbent. It can also be seen that there are no new adsorption bands after the experiment.

Figure 9 shows the IR spectra of the CaCO$_3$ before and after the adsorption experiments. Similar to Na$_2$CO$_3$, the adsorption band at 1417, 877 and 702 cm^{-1} for the O-C-O bond becomes weaker. However, two bands appear at 820 cm^{-1} and 699 cm^{-1}, which are attributed to the IR adsorption of CaCl$_2$, suggesting the formation of CaCl$_2$ following the adsorption of chlorobenzene.
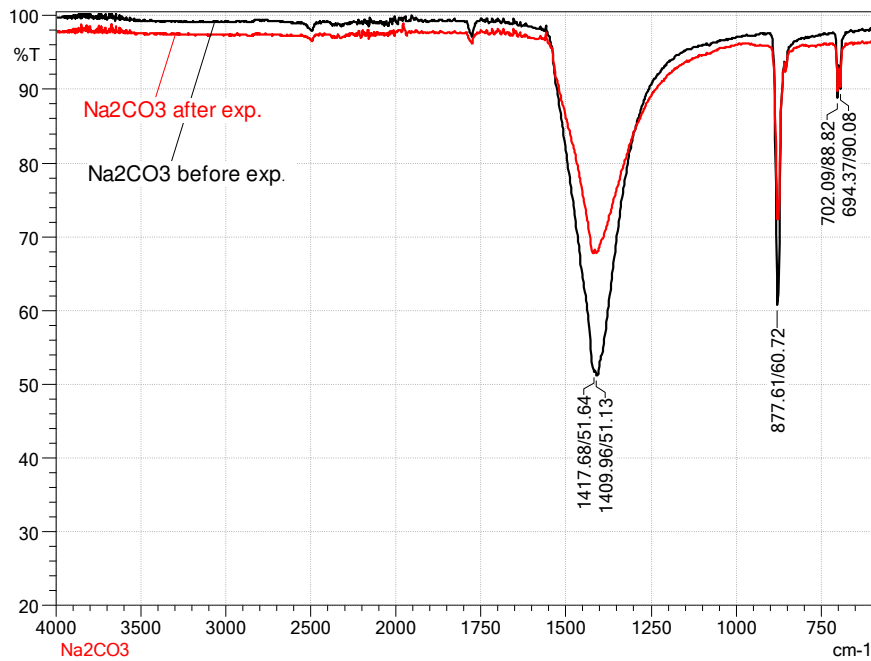

Figure 8. IR spectra of the adsorbent Na$_2$CO$_3$ before and after adsorption of chlorinated hydrocarbons. The adsorbate was chlorobenzene in isooctane (10000ppm by wt.).
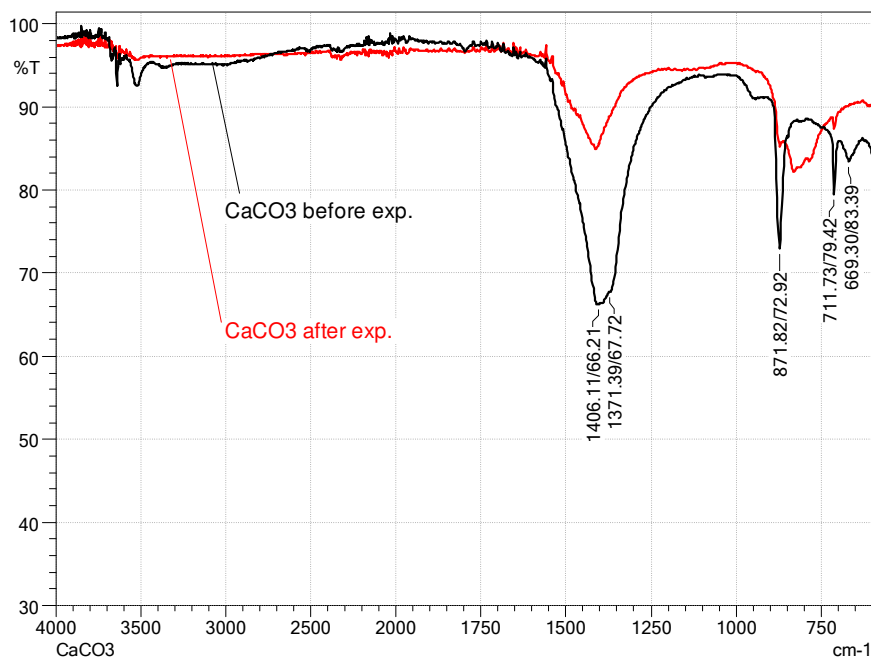
Figure 9. IR spectra of the adsorbent $CaCO_3$ before and after adsorption of chlorinated hydrocarbons. The adsorbate was chlorobenzene in isooctane (10000 ppm by wt.).

The alkali after the adsorption experiment were further characterised using XRD. The XRD pattern is shown in Figure 10 for the Na_2CO_3 and in Figure 11 for $CaCO_3$ after adsorption of chlorobenzene. It can be seen that the XRD pattern contains both diffraction peaks for Na_2CO_3 and NaCl for Na_2CO_3 as the adsorbent, and $CaCO_3$ and $CaCl_2$ for $CaCO_3$ as the adsorbent. Clearly, the Na_2CO_3 phase is partially converted to NaCl, which is consistent with the IR analysis, since NaCl is IR transparent. The $CaCO_3$ is converted to $CaCl_2$, which is also consistent with the IR analysis.
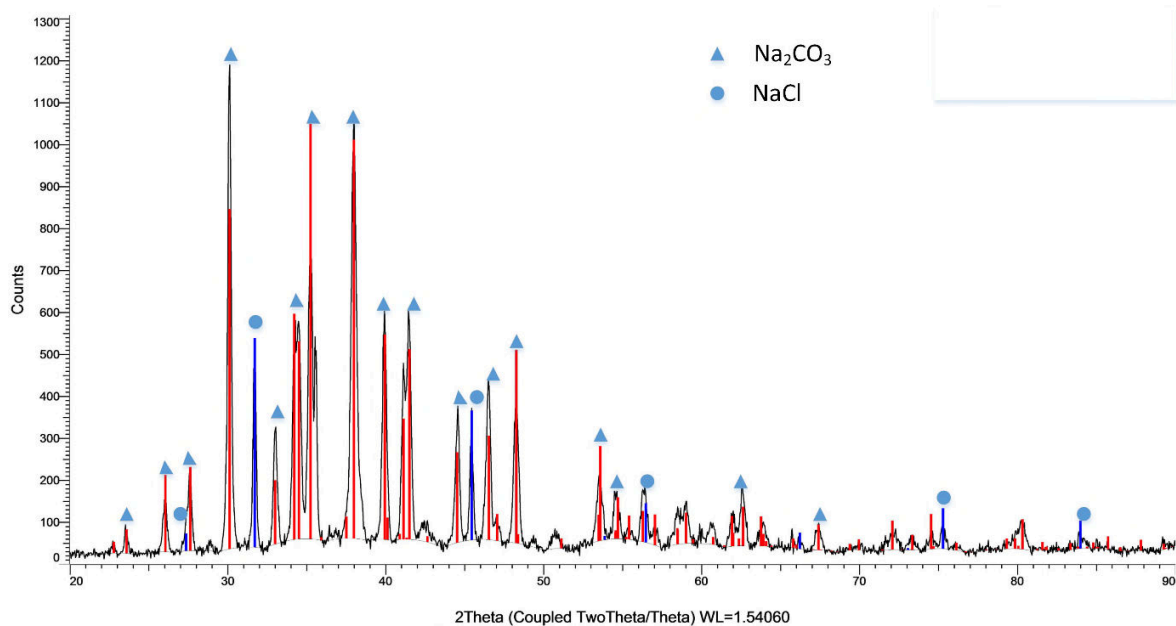
Figure 10. XRD diffraction pattern for Na_2CO_3 after absorption of chlorobenzene.
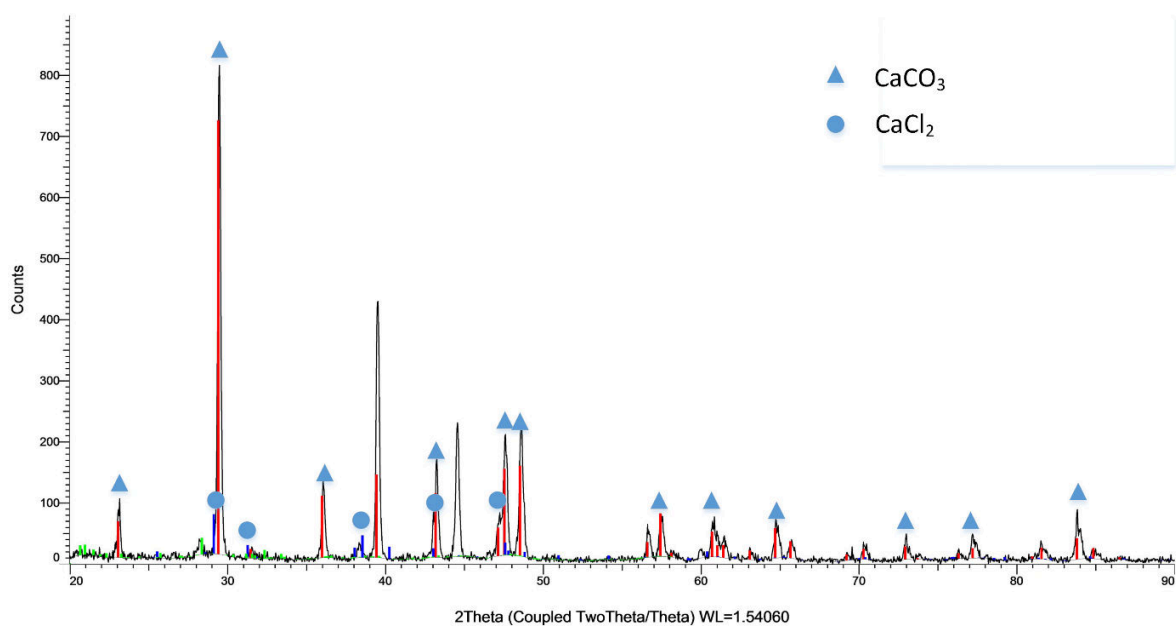

Figure 11. XRD diffraction pattern for $CaCO_3$ after absorption of chlorobenzene.

The XRD diffraction patterns of the fresh and used alumina are shown in Figure 12. The fresh alumina has three main broad diffraction peaks at 37.59°, 44.48°, 45.84°, and 67.00°, which are

characteristic of γ-alumina.[30] The XRD diffraction pattern of the alumina used with Na_2CO_3 has characteristic diffraction peaks of alumina. However, some distinguished carbon diffraction peaks at 27.28°, 31.63°, 45.33°, 75.16°, and 78.16° is superposed over alumina.[31] The alumina used with $CaCO_3$ also has characteristic diffraction peaks of alumina, but has much weak carbon peaks superposed over alumina, which may be due to the less carbon on the surface originating from coke produced from hydrocarbon cracking.[32] . The XRD pattern of the used and fresh alumina indicates that the structure of alumina is not changed during the adsorption.
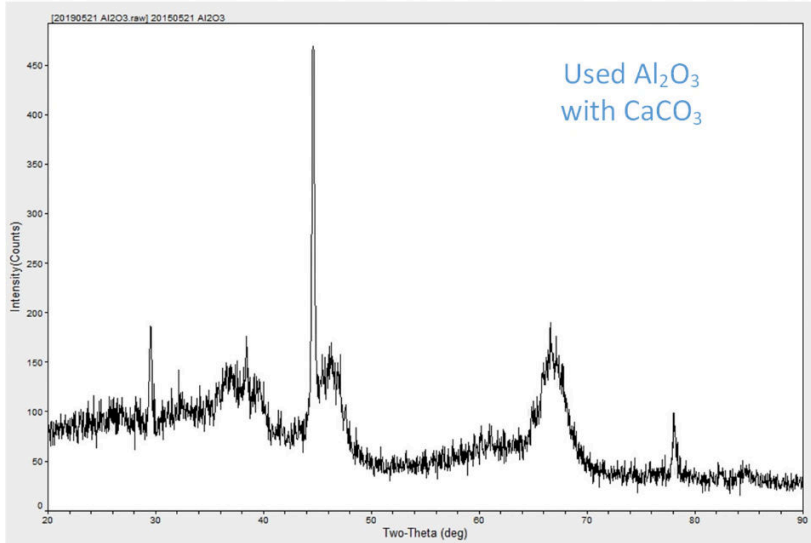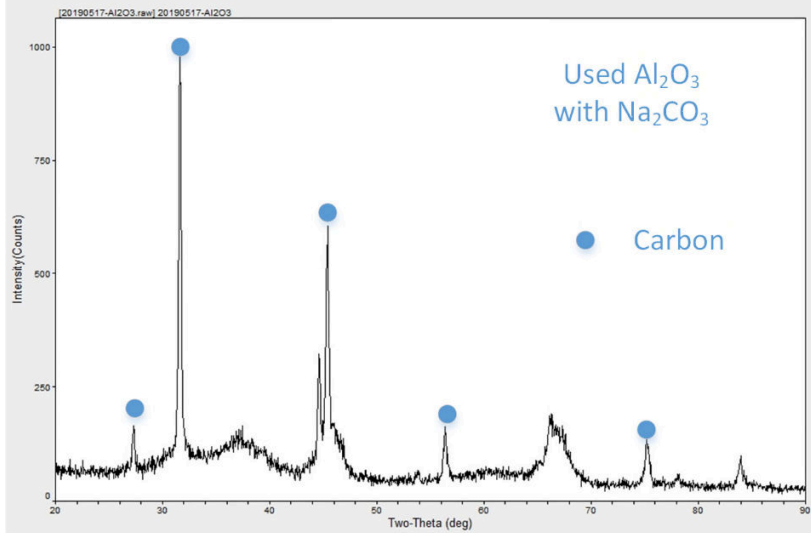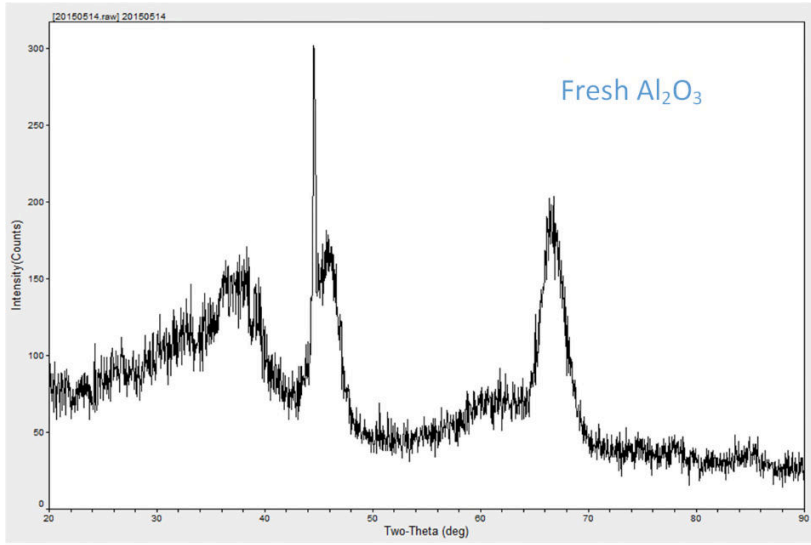
Fresh Al$_2$O$_3$

Used Al$_2$O$_3$
with Na$_2$CO$_3$

● Carbon

Used Al$_2$O$_3$
with CaCO$_3$

Figure 12. XRD patterns of the fresh and used alumina with Na_2CO_3 and $CaCO_3$ absorbents.

Mechanism of the adsorption of chlorobenzene

The results showed that both Na_2CO_3 and $CaCO_3$ alone cannot dechlorinate chlorobenzene at a temperature below 550°C, which is consistent with the literature reports.[27, 29] In contrast, the dechlorination occurred at much higher temperatures of 700 to 900°C in those reports.[27, 29] In addition, this work showed that alumina alone cannot crack chlorobenzene below 550°C. However, the dechlorination reaction occurred when alumina and an alkali were used together.

It is well known that alumina can catalyse the cracking of hydrocarbons via a carbocation mechanism.[28] The cracking of isooctane can be seen in the chromatogram for the adsorption of chlorobenzene at 450°C as shown in Figure 3. The dechlorination of chlorobenzene is promoted in this ionic environment, implying that the breaking of C-Cl bond has also an ionic nature, and consequently, can be facilitated by the ion species formed from the isooctane cracking on the alumina.

Furthermore, the adsorption capacity of the alkali adsorbents (Na_2CO_3 and $CaCO_3$) toward chlorobenzene is much smaller when compared with the adsorption of 2-chloroethylbenzene. This indicates that the interior of the alkalis can be used for the adsorption of 2-chloroethylbenzene, but not for chlorobenzene. The dechlorination of chlorobenzene proceeded only on the surface.

The sizes of the molecules involved in the adsorption were estimated according to their densities and molar masses using Equation 2, and the results are presented in Table 1.

$$D = \sqrt[3]{\frac{M}{\rho N_A}} \qquad (2)$$

Where M is the molar mass (kg/kmol), ρ is the density (kg/m^3), and N_A is the Avogadro constant (6.023 x 10^{23} /mol).

**Table2**. Estimated molecular size of the chlorinated hydrocarbons and HCl.

Molecules	Density (kg/m^3)	Molar mass (kg/kmol)	Volume/molecule (Å^3)	Molecule size (Å)
chlorobenzene	1110	112.56	168.36	5.52
2-chlorobutane	873	92.57	176.05	5.60
2-chloroethylbenzene	1069	140.61	218.39	6.02
HCl	1490	36.46	40.63	3.43

As shown in Table 2, the three chlorinated hydrocarbons have similar size, while the size of HCl is about half of those chlorinated hydrocarbons. If the adsorption of all these chlorinated hydrocarbons proceeded by direct interaction with the adsorbents, their adsorption behaviour would be similar. The much greater adsorption capacity for both 2-chlorobutane and 2-chloroethylbenzene can be attributed to the rapid alkali adsorption of HCl formed via dehydrochlorination, while the dechlorination of chlorobenzene occurred by direct interaction of the alkali and chlorobenzene, which was not able to access the interior of the alkali because of its larger molecular size compared with HCl. It can be inferred that HCl would be able to access the interior of the adsorbents, and this can be observed by Torres et al.'s work.[33]

Based on the above inference, the dechlorination of chlorobenzene in the presence of alumina and isooctane is shown in Scheme 5. At first, a carbocation species R$^+$ formed from cracking isooctane attaches the negatively charged chlorine of chlorobenzene, making the carbon of the C-Cl bond more positively charged, which facilitates the attacking of the negatively charged oxygen of Na$_2$CO$_3$, to break the C-Cl bond forming NaCl and a phenyl cation. The pathway of forming R-Cl and a phenyl cation should not occur since this will lead to the same reaction mechanism as that of aliphatic chlorinated hydrocarbons, but on the contrary thus occurs according to our work. The phenyl cation may then abstract a surface hydroxyl group on the surface of the adsorbent to form phenol or abstract hydrogen from isooctane to form benzene. The hydroxyl group may come from the moisture on the surface, since the production of phenol disappeared at later stages of the adsorption, as shown in Figure S7 for the evolution of benzene and phenol in the adsorption. The overall effect of this mechanism is similar to the Cl$^-$/O^2 ion

exchange mechanism proposed by Li et al.[27] , but the authors did not illustrate how the exchange took place.

As shown in Table 1, the calculation of the mass of the Na_2CO_3 adsorbent according to a simple exchange of O and Cl does not match the actual mass change. This indicates that some further reaction such as formation of CO_2 may occur after replacement of one oxygen of Na_2CO_3 with chlorine.
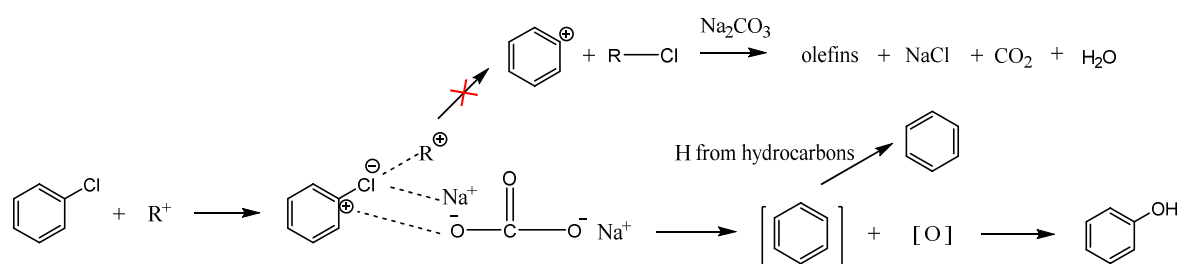
Scheme 5. Proposed reaction mechanism for dechlorination of chlorobenzene

This mechanism has strong implications for the removal of chlorine from the pyrolysis of mixed plastics containing PVC. This study indicates that the key to dechlorinate pyrolysis vapour is to dechlorinate aromatic chlorinated hydrocarbons, which proceeds on the surface of adsorbents and requires higher temperature. The dechlorination of aliphatic chlorinated hydrocarbons is relatively easy, which can be implemented at much lower temperature, and has a nature of acid-base neutralization, as shown in Schemes 3 and 4. It can be inferred that alkaline substances supported on a solid acidic carrier with large pore size may be used to remove both aliphatic and aromatic chlorinated hydrocarbons. For example, the pore size of the adsorbent should be greater than 5.5 Å for adsorption of chlorobenzene, such as 10A or mesoporous zeolites used as the carrier.

CONCLUSIONS

In this work, the mechanism of dechlorination of chlorinated hydrocarbons is investigated by the adsorption on alkali adsorbents. 2-Chlorobutane, 2-chloroethylbenzene and chlorobenzene doped in isooctane were used to model the pyrolysis vapour containing chlorinated hydrocarbons. The following conclusions can be drawn.

Two mechanisms are operating for the dechlorination of chlorinated hydrocarbons. For aliphatic chlorinated hydrocarbons that contain aliphatic hydrogen adjacent to the chlorine atom, the pathway for dechlorination is via the dehydrochlorination of the chlorinated compound resulting in the formation of olefins and HCl. The reaction is driven to completion by the *in situ* removal of the HCl through its reaction with the alkali in the adsorbent. After adsorption, the alkali is converted to the corresponding metal chloride. This reaction can be carried out as low as 180°C.

The dechlorination of aromatic chlorinated hydrocarbons, such as chlorobenzene is much more difficult than that of aliphatic chlorinated hydrocarbons. In the presence of alumina and isooctane, the dechlorination can be achieved at around 300°C, due to the enhancing effect of the ionic intermediate produced by cracking of the hydrocarbon.

ACKNOWLEDGEMENTS

REFERENCES

1.   Kaminsky, W., Chemical recycling of mixed plastics by pyrolysis. *Adv. Polym. Technol.* **1995,** *14*, 337-344, DOI: 10.1002/adv.1995.060140407

2.   Fukushima, M.; Shioya, M.; Wakai, K.; Ibe, H., Toward maximizing the recycling rate in a Sapporo waste plastics liquefaction plant. *J. Mater. Cycles Waste Manag.* **2009,** *11*, 11-18, DOI: 10.1007/s10163-008-0212-6

3.   Kumagai, S.; Toshioka, T., Feedstock recycling via waste plastic pyrolysis. *J. Japan Pet. Inst.* **2016,** *59*, 243-253, DOI: 10.1627/jpi.59.243

4.   Westerhout, R. W. J.; van Koningsbruggen, M. P.; van der Ham, A. G. J.; Kuipers, J. A. M.; van Swaaij, W. P. H., Techno-economic evaluation of high temperature pyrolysis processes for mixed plastic waste. *Trans. Inst. Chem. Eng.* **1998,** *76*, 427-439, DOI: 10.1205/026387698524857

5.   Fonseca, J. D.; Grause, G.; Kameda, T.; Yoshioka, T., Effects of steam on the thermal dehydrochlorination of poly(vinylchloride) resin andflexible poly(vinyl chloride) under atmosphericpressure. *Polym. Degrad. Stab.* **2015,** *117*, 8-15, DOI: 10.1016/j.polymdegradstab.2015.03.011

6.   Hapipi, A. M.; Suda, H.; Uddin, M. A.; Kato, Y., Dechlorination of polyvinyl chloride under superheated steam with catalysts and adsorbents. *Energy Fuels* **2018,** *32*, 7792-7799, DOI: 10.1021/acs.energyfuels.8b00838

7.   Nishibata, H.; Uddin, M. A.; Kato, Y., Simultaneous degradation and dechlorination of poly (vinyl chloride) by a combination of superheated steam and CaO catalyst/adsorbent. *Polym. Degrad. Stab.* **2020,** *179*, Article 109225, DOI: 10.1016/j.polymdegradstab.2020.109225

8.   Kameda, T.; Ono, M.; Grause, G.; Mizoguchi, T.; Yoshioka, T., Ball Mill-Assisted Dechlorination of Flexible and Rigid Poly(vinyl chloride) in NaOH/EG Solution. *Ind. Eng. Chem. Res.* **2008,** *47*, 8619-8624, DOI: 10.1021/ie8006819

9.   Yoshioka, T.; Kameda, T.; Imai, S.; Okuwaki, A., Dechlorination of poly(vinyl chloride) using NaOH in ethylene glycol under atmospheric pressure. *Polym. Degrad. Stab.* **2008,** *93*, 1138-1141, DOI: 10.1016/j.polymdegradstab.2008.03.007

10.   Zakharyan, E. M.; Petrukhina, N. N.; Maksimov, A. L., Pathways of Chemical Recycling of Polyvinyl Chloride: Part 1. *Russ. J. Appl. Chem.* **2020,** *93*, 1271-1313, DOI: 10.1134/S1070427220090013

11.   Hinz, B.; Hoffmockel, M.; Pohlmann, K.; Schadel, S.; Schimmel, I.; Sinn, H., Dehalogenation of pyrolysis products. *J. Anal. Appl. Pyrolysis* **1994,** *30*, 35-46, DOI: 10.1016/0165-2370(94)00800-0

12.   Cho, M.-H.; Jung, S.-H.; Kim, J.-S., Pyrolysis of mixed plastics wastes for the recovery of benzene, toluene and xylene aromatics in a fluidized bed and chlorine removal by applying various additives. *Energy Fuels* **2010,** *24*, 1389-1395, DOI: 10.1021/ef901127v

13.   Bhaskar, T.; Matsui, T.; Kaneko, J.; Uddin, M. A.; Muto, A.; Sakata, Y., Novel calcium based sorbent (Ca-C) for the dehalogenation (Br, Cl) process during halogenated mixed plastic (PP/PE/PS/PVC and HIPS-Br) pyrolysis. *Green Chem.* **2002,** *4*, 372-375, DOI: 10.1039/B203745A

14.   Bie, R.; Li, S.; Yang, L., Reaction mechanism of CaO with HCl in incineration of wastewater in fluidized bed. *Chem. Eng. Sci.* **2005,** *60*, 609-616, DOI: 10.1016/j.ces.2004.08.022

15.   Daoudi, M.; Walters, J. K., The reaction of HCl gas with calcined commercial limestone particles: The effect of particle size. *Chem. Eng. J.* **1991,** *47*, 11-16, DOI: 10.1016/0300-9467(91)85002-D

16.   Lingaiah, N.; Uddin, M. A.; Muto, A.; Sakata, Y.; Imai, T.; Murata, K., Catalytic dechlorination of chloroorganic compounds from PVC-containing mixed plastic-derived oil. *Appl. Catal., A* **2001,** *207*, 79-84, DOI: 10.1016/S0926-860X(00)00656-6

17.   Lingaiah, N.; Lingaiah, N.; Uddin, M. A.; Morikawa, K.; Muto, A.; Murata, K.; Sakata, Y., Catalytic dehydrochlorination of chloro-organic compounds from PVC containing waste plastics derived fuel oil over FeCl2/SiO2 catalyst. *Green Chem.* **2001,** *3*, 74-75, DOI: 10.1039/B009471O

18.   Lingaiah, N.; Uddin, M. A.; Muto, A.; Imai, T.; Sakata, Y., Removal of organic chlorine compounds by catalytic dehydrochlorination for the refinement of municipal waste plastic derived oil. *Fuel* **2001,** *80*, 1901-1905, DOI: 10.1016/S0016-2361(01)00046-1

19.   Uddin, M. A.; Sakata, Y.; Shiraga, Y.; Muto, A.; Katsuhide, M., Dechlorination of chlorine compounds in poly(vinyl chloride) mixed plastics derived oil by solid sorbents. *Ind. Eng. Chem. Res.* **1999,** *38*, 1406-1410, DOI: 10.1021/ie980445k

20.   Lopez-Urionabarrenechea, A.; Marco, I.; Caballero, B. M.; Laresgoiti, M. F.; Adrados, A., Upgrading of chlorinated oils coming from pyrolysis of plastic waste. *Fuel Process. Technol.* **2015,** *137*, 229-239, DOI: 10.1016/j.fuproc.2015.04.015

21.   McNeill, I. C.; Memetea, L.; Cole, W. J., A study of the products of PVC thermal degradation. *Polym. Degrad. Stab.* **1995,** *49*, 181-191, DOI: 10.1016/0141-3910(95)00064-S

22.   Miranda, R.; Yang, J.; Roy, C.; Vasile, C., Vacuum pyrolysis of PVC. I. Kinetic study. *Polym. Degrad. Stab.* **1999,** *64*, 127-144, DOI: 10.1016/S0141-3910(98)00186-4

23.   Miranda, R.; Pakdel, H.; Roy, C.; Hans, D.; Vasile, C., Vacuum pyrolysis of PVC II: Product analysis. *Polym. Degrad. Stab.* **1999,** *66*, 107-125, DOI: 10.1016/S0141-3910(01)00066-0

24.   Bej, S. K.; Dalai, A. K.; Maity, S. K., Effect of diluent size on the performance of a micro-scale fixed bed multiphase reactor in up flow and down flow modes of operation. *Catal. Today* **2001,** *64*, 333-345, DOI: 10.1016/S0920-5861(00)00536-8

25.   Moene, R.; Makkee, M.; Moulijn, J. A., High surface area silicon carbide as catalyst support characterization and stability. *Appl. Catal., A* **1998,** *167*, 321-330, DOI: 10.1016/S0926-860X(97)00326-8

26.   Cullis, C. F.; Manton, J. E., The pyrolysis of chlorobenzene. *J. Chem. Soc. Faraday Trans.* **1958,** *54*, 381-389, DOI: 10.1039/TF9585400381

27.   Li, Y.-X.; Li, H.; Klabunde, K. J., Destructive adsorption of chlorinated benzenes on ultrafine (nanoscale) particles of magnesium oxide and calcium oxide. *Environ. Sci. Technol.* **1994,** *28*, 1248-1253, DOI: 10.1021/es00056a011

28.   Westrich, T. A.; Chen, X.; Schwank, J. W., Isooctane decomposition and carbon deposition over ceria-zirconia supported nickel catalysts. *Appl. Catal., A* **2010,** *386*, 83-93, DOI: 10.1016/j.apcata.2010.07.029

29.   Parrett, J. W.; Sumner, J. P.; Devore, T. C., Reaction between chlorocarbon vapors and sodium carbonate. *Environ. Sci. Technol.* **1999,** *33*, 1691-1696, DOI: 10.1021/es980077b

30.   Rozita, Y.; Brydson, R.; Scott, A. J., An investigation of commercial gamma-Al_2O_3 nanoparticles. *J. Phys. Conf. Ser.* **2009,** *241*, article # 012096, DOI: 10.1088/1742-6596/241/1/012096

31.   Ungar, T.; Gubicza, J.; Ribarik, G.; Pantea, C.; Zerda, T. W., Microstructure of carbon blacks determined by X-ray diffraction profile analysis. *Carbon* **2002,** *40*, 929-937, DOI: 10.1016/S0008-6223(01)00224-X

32.   Sinfelt, J. H.; Rohrer, J. C., Cracking of hydrocarbons over a promoted alumina catalyst. *J. Phys. Chem.* **1962,** *66*, 1559-1560, DOI: doi.org/10.1021/j100814a516

33.   Torres, D.; Jiang, Y.; Sanchez-Monsalve, D. A.; Leeke, G. A., Hydrochloric acid removal from the thermogravimetric pyrolysis of PVC. *J. Anal. Appl. Pyrolysis* **2020,** *149*, #104831, DOI: 10.1016/j.jaap.2020.104831

TOC/GRAPHIC ABSTRACT
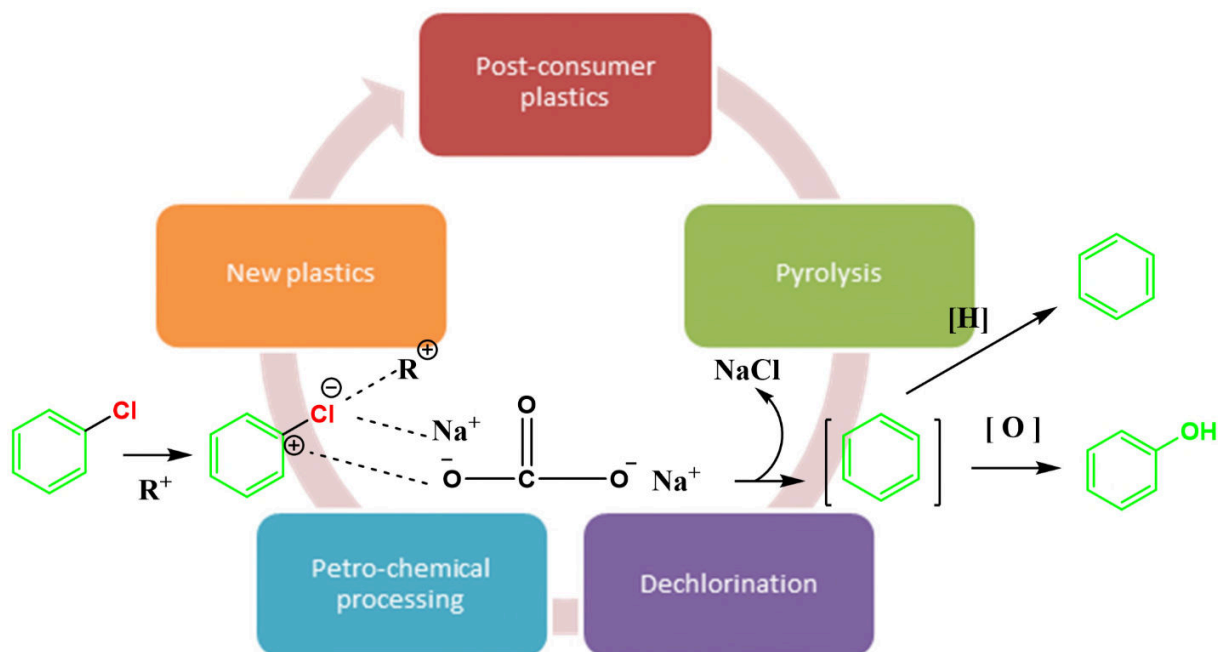
SYNOPSIS

The mechanism of dechlorination of chlorinated hydrocarbons was explored for producing qualified plastic oil as petrochemical feedstock.